



## LJMU Research Online

**Ross, S, Murphy, MF, Lilley, F, Lalor, MJ and Burton, DR**

**Single-beam three-dimensional optical trapping at extremely low insertion angles via optical fiber optimization**

<http://researchonline.ljmu.ac.uk/id/eprint/314/>

### Article

**Citation** (please note it is advisable to refer to the publisher's version if you intend to cite from this work)

**Ross, S, Murphy, MF, Lilley, F, Lalor, MJ and Burton, DR (2014) Single-beam three-dimensional optical trapping at extremely low insertion angles via optical fiber optimization. Optical Engineering, 53 (8). ISSN 0091-3286**

LJMU has developed **LJMU Research Online** for users to access the research output of the University more effectively. Copyright © and Moral Rights for the papers on this site are retained by the individual authors and/or other copyright owners. Users may download and/or print one copy of any article(s) in LJMU Research Online to facilitate their private study or for non-commercial research. You may not engage in further distribution of the material or use it for any profit-making activities or any commercial gain.

The version presented here may differ from the published version or from the version of the record. Please see the repository URL above for details on accessing the published version and note that access may require a subscription.

For more information please contact [researchonline@ljmu.ac.uk](mailto:researchonline@ljmu.ac.uk)

<http://researchonline.ljmu.ac.uk/>

# Optical Engineering

OpticalEngineering.SPIEDigitalLibrary.org

## **Single-beam three-dimensional optical trapping at extremely low insertion angles via optical fiber optimization**

Steven Ross  
Mark F. Murphy  
Francis Lilley  
Michael J. Lalor  
David R. Burton

**SPIE.**

# Single-beam three-dimensional optical trapping at extremely low insertion angles via optical fiber optimization

Steven Ross,<sup>a,\*</sup> Mark F. Murphy,<sup>a,b</sup> Francis Lilley,<sup>a</sup> Michael J. Lalor,<sup>a</sup> and David R. Burton<sup>a</sup>

<sup>a</sup>Liverpool John Moores University, Faculty of Technology and Environment, General Engineering Research Institute, Byrom Street, Liverpool, L3 3AF, United Kingdom

<sup>b</sup>Liverpool John Moores University, The School of Pharmacy and Biomolecular Sciences, Byrom Street, L3 3AF, United Kingdom

**Abstract.** Employing optical fiber to deliver the trapping laser to the sample chamber significantly reduces the size and costs of optical tweezers (OT). The utilization of fiber decouples the OT from the microscope, providing scope for system portability, and the potential for uncomplicated integration with other advanced microscopy systems. For use with an atomic force microscope, the fiber must be inserted at an angle of 10 deg to the plane of the sample chamber floor. However, the literature states that optical trapping with a single fiber inserted at an angle  $\leq 20$  deg is not possible. This paper investigates this limitation and proposes a hypothesis that explains it. Based on this explanation, a tapered-fiber optical tweezer system is developed. This system demonstrates that such traps can indeed be made to function in three-dimensions (3-D) at insertion angles of  $\leq 10$  deg using relatively low optical powers, provided the fiber taper is optimized. Three such optimized tapered fiber tips are presented, and their ability to optically trap both organic and inanimate material in 3-D is demonstrated. The near-horizontal insertion angle introduced a maximum trapping range (MTR). The MTR of the three tips is determined empirically, evaluated against simulated data, and found to be tunable through taper optimization. © 2014 Society of Photo-Optical Instrumentation Engineers (SPIE) [DOI: 10.1117/1.OE.53.8.085107]

Keywords: optical trapping; tapered optical fiber; applied optics; micro-optics; microlens.

Paper 140161 received Jan. 28, 2014; revised manuscript received Jun. 30, 2014; accepted for publication Jul. 22, 2014; published online Aug. 21, 2014.

## 1 Introduction

We aim here to develop an optical trapping system to aid our investigations into the mechanical properties of cells.<sup>1-6</sup> We currently employ atomic force microscopy (AFM) to carry out force-indentation experiments on adherent cells. However, we would also like to use AFM to study the force response of nonadherent cells, e.g., blood cells. In order to achieve this, the nonadherent cells would be required to be held in place while the AFM cantilever is brought into contact with them. This is one of the driving forces behind the design of our optical trap. The system should be physically decoupled from the microscope and exhibit a certain degree of portability to ensure its interoperability with other such microscopy systems. With this in mind, an optical fiber based system configuration has been proposed here.

Existing literature suggests that full three-dimensional (3-D) optical trapping is not possible using a single optical fiber inserted at an angle  $< 20$  deg to the plane of the sample chamber floor.<sup>7</sup> Previously, single optical fiber traps have also shown a significant reduction of trapping efficiency at insertion angles of  $< 40$  deg to the plane of the sample chamber.<sup>8</sup> To date, these limitations have not been investigated in order to discover their cause. This paper investigates these limitations and proposes a hypothesis that is based on the geometric profile of the optical fiber's distal end. Consequently, a solution is proposed whereby the geometry of the tapered optical fiber's distal end is optimized to allow 3-D optical trapping at an insertion angle of 10 deg for silica

particles 3  $\mu\text{m}$  in diameter. To the authors' knowledge, this is the first time that a fiber-based single-beam 3-D optical trapping system has been employed at such extremely low insertion angles for the particle sizes given above.

The authors are not claiming to have developed a new method for fiber taper fabrication here. Indeed, the method proposed in Ref. 9 was deemed to be an ideal solution for optical trapping of small particles at low insertion angles. However, it was found that replication of this work could not be achieved. An alternative method has been proposed in Ref. 10. By applying this latter dual heating method, the authors found that it was possible to achieve 3-D optical trapping, initially at an insertion angle of 45 deg, using low optical powers. At an insertion angle of 10 deg, 3-D optical trapping was still achieved. However, this was possible only when using exceptionally high optical output powers that were in excess of 500 mW. It was this finding that led to the hypothesis that will be described later in Sec. 5—a finding that spawned the development of the three optimized tapered fiber tips that are capable of 3-D optical trapping at extremely low insertion angles, using optical output powers of  $< 20$  mW.

The near horizontal orientation of the fiber has led to observable changes in the trapping dynamics when compared to those encountered at larger insertion angles. One such change was in the form of a maximum trapping range. Computer simulations of the optical trapping range for similar shaped optical fiber tapers have previously been performed.<sup>10</sup> However, since optical trapping at

\*Address all correspondence to: Steven Ross, E-mail: [s.ross@2002.ljmu.ac.uk](mailto:s.ross@2002.ljmu.ac.uk)

insertion angles  $<20$  deg have previously been perceived to be unattainable, determining these results experimentally has thus far been neglected.

## 2 Origins of Optical Trapping

The origins of optical trapping can be traced back to 1969 when Ashkin initiated investigations into the effects of electromagnetic radiation pressure upon microscopic particles.<sup>11</sup> It was during these experiments that unusual and extraordinary phenomena were observed. These observations led to a full appreciation of the optical forces at play during the interaction between light and matter, which led Ashkin to develop the first optical trapping systems.<sup>11,12</sup> In 1986, Ashkin developed the first single-beam, gradient force 3-D optical trap, which has since become known as optical tweezers.<sup>13</sup> Since then, these initial optical trapping systems have been built upon and improved, offering systems that provide multiple and flexible optical trapping sites.<sup>14-21</sup>

Optical traps are capable of generating optical forces  $>100$  pN with subnanometer resolution,<sup>22</sup> while simultaneously measuring the displacement of particles of sizes ranging between the Rayleigh and Mie regimes. As a consequence, optical trapping systems have since become invaluable tools within the physical<sup>23,24</sup> and biological sciences.<sup>25-28</sup> A full description of the theory, design, and construction of optical tweezers has been well covered in the literature and the reader is guided to Refs. 29-34.

### 2.1 Optical Fiber Based Optical Trapping System Configurations

The first optical fiber based optical trapping system was developed in 1993 in an effort to reduce both the system size and building costs. This simple system comprised two counterpropagating and cleaved optical fibers.<sup>35</sup> However, this configuration lacked stability in the longitudinal direction, leading to two different approaches being taken to address the issue. The first employed tapered hemispherical lenses fabricated onto the end of the optical fibers.<sup>36-39</sup> The second setup utilized a further two optical fibers, which were added to the system to provide a cross-hair configuration.<sup>40,41</sup>

The hemispherical lensed approach failed to provide 3-D trapping using a single fiber, since the necessary high numerical aperture could not be achieved. In an attempt to replicate optical tweezers, the first single optical fiber based full 3-D optical trap was developed.<sup>42</sup>

3-D trapping was claimed to have been achieved using a tapered optical fiber.<sup>43</sup> A description of the trapping experiment in a prior publication suggests that it was capable of only two-dimensional (2-D) trapping.<sup>8</sup> An axicon lens was fabricated directly onto the end of a single-mode fiber (SMF) using focused ion beam (FIB) lithography to create a Bessel mode beam output for optical trapping.<sup>44</sup>

A single-beam 3-D optical trap, with a trapping efficiency that was an order of magnitude less than that of the optical tweezers system, was designed by tapering a single-mode optical fiber using a heating and drawing method.<sup>10</sup> The trapping efficiency of 3-D optical fiber trapping systems was improved using an FIB milling machine to make incisions to the optical fiber core at its end-face, the result of which is that the output from either a four fiber bundle or

a fiber with an annular core is redirected to a centralized focal spot.<sup>45-48</sup>

Single-fiber 3-D trapping was demonstrated using a custom-built optical fiber consisting of four cores that were tapered by chemical etching. The thin taper was then melted using an electric arc to cause a lens effect.<sup>49</sup> A single-fiber 3-D optical trap was produced by chemically etching the end of an SMF to form a taper.<sup>7</sup> However, no attempt was made by the author to trap at insertion angles  $<20$  deg due to the perceived notion that it was not possible.

### 2.2 Limitations and Challenges of Using Optical Fiber

Optical fiber based systems offer certain advantages, such as reduced size and building costs. However, they also possess limitations when compared to classical systems, such as a reduction in trapping efficiency.<sup>10</sup> Although this limitation has been eradicated with novel fiber modifications, the requirement for intricate shaping of the fiber end-face can only be achieved using expensive equipment such as an FIB milling machine.<sup>44,45,47,48</sup> A FIB milling machine can cost in the region of £400,000. Alternative methods for shaping of the fiber, such as chemical etching, require the use of harmful and toxic chemicals,<sup>7</sup> while other configurations require the use of specialized optical fibers,<sup>45-49</sup> a factor that could also lead to increased system cost.

The heating and drawing method provides a nonhazardous and relatively low-cost option to focus the exiting laser light. The cost of the P2000/F micropipette puller used here is 50 times less than an FIB milling machine. For these reasons and because it is already a proven method that permits 3-D optical trapping,<sup>10</sup> a tapered fiber configuration was selected for this project.

Additionally, this method maintains the optical fiber's integrity as the core/cladding ratio is maintained. This is an important factor when one considers the laser light's mode of transport along the fiber is due to total internal reflection (TIR).<sup>50</sup> Furthermore, this method can be performed relatively quickly while still offering a certain degree of repeatability. These are desirable characteristics when one considers that the fragile tapered optical fiber tips can be easily subjected to damage.

The inability of fiber based systems to trap at insertion angles of  $<20$  deg to the microscope sample chamber<sup>7</sup> was the most significant challenge to this project. The intended integration of the tapered optical fiber trapping



**Fig. 1** Asylum research molecular force probe three-dimensional (3-D) atomic force microscope head that houses the optical lever detection system located above the microscope's sample chamber.

system with our AFM (Asylum Research Molecular Force Probe atomic force microscope) requires the insertion angle of the fiber's distal end to be  $\leq 10$  deg. This would allow the fiber a clear passage under the AFM head, which is shown in Fig. 1, permitting the delivery of the laser light to the sample chamber of the microscope.

### 3 Tapered Fiber Optic Tweezers System Setup

The basic setup of the tapered fiber optic tweezers (T-FOTs) system is shown in Fig. 2. The laser source is a Ventus IR diode pumped solid state neodymium-doped yttrium aluminum garnet laser. It has a variable output power of up to 3 W and a wavelength of 1064 nm (Laser Quantum, Stockport, United Kingdom). The laser is coupled into a SMF via a laser to fiber coupler (Oz Optics Ltd., Ottawa, Canada).

To eliminate burning of the optical fiber during coupling, an SMF patch cord terminated with a high-power optical fiber connector consisting of a hollow metal ferrule is employed. The output of the high-power patch cord is fusion spliced to the input of a high-power PIN InGaAs 1% inline optical tap. Fusion spliced to the output end of the inline optical tap is a 10 m length of 1060XP SMF (Thorlabs Ltd., Ely, United Kingdom) for delivery of the laser to the sample chamber. The optical tap's output voltage is received by a USB-2404-UI DAQ module (Adept Scientific, Letchworth Garden, United Kingdom) and transmitted to the custom-built PC. The output signal from the optical tap is imported into a LabView virtual instrument and provides real-time monitoring of the optical power at the sample.

The 1060XP SMF's distal end was tapered using a Sutter P2000/F micropipette puller (Intracell Ltd., Shepreth, United Kingdom) to enable focusing of the laser light. The tapered optical fiber tip can be maneuvered within the sample chamber of a GXD-30 inverted microscope (Masarek Optical Systems Ltd., Southam, United Kingdom) in the  $X$ ,  $Y$ , and  $Z$  planes. Distances of up to 5 mm of coarse travel can be achieved using three motorized compact M-110.1DG microtranslation stages configured for  $X$ ,  $Y$ , and  $Z$  axis translations. Alternatively, movement of a finer nature can be achieved over 100  $\mu\text{m}$  distances in both the  $X$  and  $Y$  directions using the P-621.2CD PIHera XY Piezo stage and using the P-621.ZCD PIHera Precision Z stage in

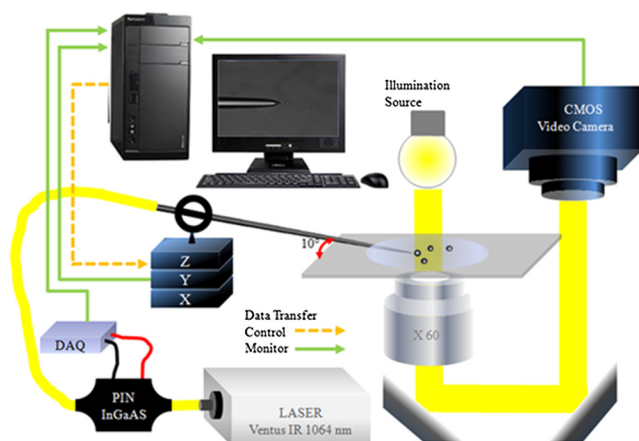


**Fig. 2** Schematic diagram showing the setup of the single tapered optical fiber tweezers system.

**Table 1** Tapered fiber optic tweezers system insertion losses.

Component	Insertion loss	Quantity	Total insertion loss
Laser to fiber coupler	1.25 dB	1	1.25 dB
HP Patch-cord	0.3 dB	1	0.3 dB
1060 XP single-mode fiber	1.5 dB/km	10 m	0.015 dB
Inline optical tap	0.15 dB	1	0.15 dB
Fusion splice	0.05 dB	2	0.1 dB
Additional losses	0.29 dB	1	0.29 dB
<b>Total system losses</b>			<b>2.855 dB</b>

the  $Z$  direction (Lambda Photometrics, Harpenden, United Kingdom). A miniature rotation stage 07 TRT 508 (CVI Laser Optics & Melles Griot, Cambridge, United Kingdom) allows changes to the insertion angle to be quickly and accurately achieved.

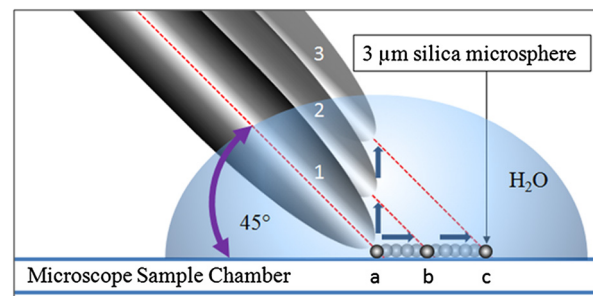
A CMOS video camera, DeltaPix Infinity X (Kane Computing Ltd., Northwich, United Kingdom), is used to monitor the microscope sample chamber, provide position detection, and record optical trapping procedures for later analysis.

Table 1 shows the insertion loss power budget for the T-FOT system. The given insertion losses for the system components are totaled to be 2.855 dB. This equates to a possible maximum output power at the sample of  $\sim 1558$  mW, which is an overall power loss of 48%. In reality, the system has a maximum power output of 1425 mW at the sample, which is a loss of 52.5%. Therefore, the actual system insertion losses are closer to 3.2 dB.

### 4 Experimental Test for 3-D Trapping

The tapered optical fiber tip is aligned within the microscope sample chamber. A sample solution of de-ionized water and 3  $\mu\text{m}$  diameter silica microspheres are added to a microscope slide. The tapered optical fiber tip is maneuvered about the sample chamber and aligned close to a microsphere. Then the laser is activated and the microsphere is observed. If the optical fiber taper is capable of only a 2-D optical trap, then it is disregarded.

The action of a 2-D optically trapped microsphere is depicted in Fig. 3. Here the optical fiber is inserted at an



**Fig. 3** The effect of optical fiber elevation on a microsphere that is optically trapped in only two dimensions.

angle of 45 deg. The fiber can be seen to be at its initial location, denoted as position (1), with the microsphere located at position (a). As the fiber is elevated to position (2), the microsphere, guided by the laser beam, is pushed away from the fiber's end-face to position (b). As the fiber is further elevated, e.g., to position (3), it becomes indistinct as it gradually moves out of the focal region of the microscope objective. However, this is not the case for the microsphere, which, as it is only trapped in 2-D, fails to be elevated and, thus, is maintained clearly in focus as it remains seated on the microscope chamber floor at position (c). Since the microsphere remains guided within the beam by the gradient force, if the optical fiber is descended back to its original position (1), then the microsphere also returns back to the origin (a).

However, if optical trapping occurs at an insertion angle of 45 deg, then that taper is subjected to further testing to validate its capability for 3-D optical trapping. This involves elevating the trapping fiber in the positive  $z$  direction. If 3-D trapping occurs, then both the fiber and the microsphere will synchronously elevate. This is detectable by both the tip and the microsphere departing from the focal plane as exhibited in Fig. 4(f).

At near horizontal insertion angles, only 3-D optical trapping can stably hold a target. The reason for this is that the fiber's orientation is such that the sample chamber floor offers almost no resistance and, therefore, the particle will be propelled in the direction of the laser beam's propagation rather than being optically trapped.

#### 4.1 Result: Experimental 3-D Optical Trapping Test

Figure 4 shows images [Figs. 4(a) to 4(g)] taken from the video sequence of a 3-D optical trapping test experiment, recorded at 30 fps using the DeltaPix Infinity X CMOS video camera. The images show the tapered fiber optic tip number 44 at an insertion angle of 45 deg to the sample chamber. At the end of the tapered fiber optic tip is an optically trapped 3- $\mu\text{m}$  silica microsphere labeled A. The 3- $\mu\text{m}$  silica microsphere labeled B in the image sequences is free to drift in the surrounding medium (water). Sphere A is moved in an anticlockwise direction around the reference sphere B.

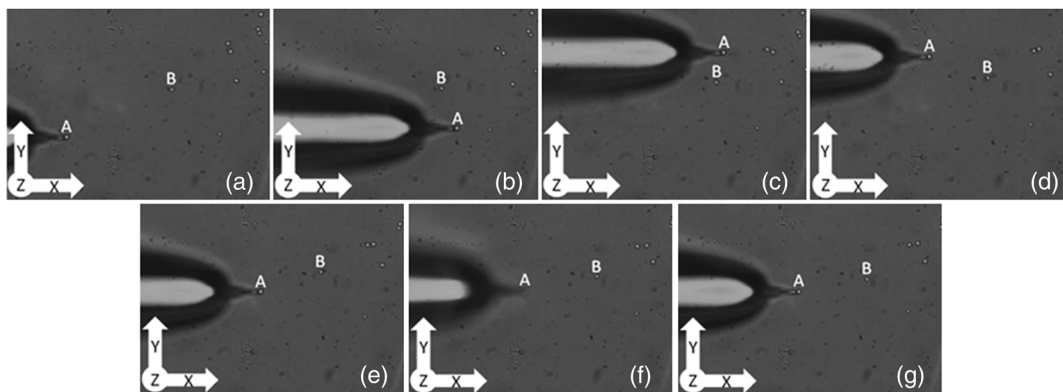


**Fig. 4** Tip number 44 3-D optical trapping at 45-deg insertion angle; X-Y trapping (a) the tapered fiber probe and 3- $\mu\text{m}$ -diameter silica microsphere trapped at the fiber end. (b) to (e) The piezo translation stages move the tapered fiber tip, directing sphere A in an anticlockwise direction around sphere B, in the directional sequence  $+X$ ,  $+Y$ ,  $-X$ ,  $-Y$ . (f) and (g) Z-Trapping. (f) The trapping fiber is moved in the  $+Z$  direction and both the fiber and the silica sphere can be seen to be out of focus. (g) The trapping fiber is moved in the  $-Z$  direction and both are now seen to be back in focus.

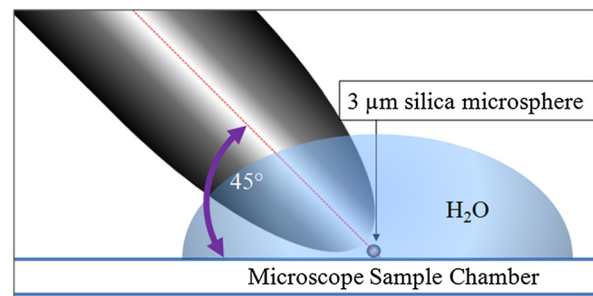
The directional sequence of the tapered fiber optic tip is (a) origin, (b)  $+X$  direction, (c)  $+Y$  direction, (d)  $-X$  direction, (e)  $-Y$  direction, (f)  $+Z$  direction, (g)  $-Z$  direction. When the translation stage was moved in the  $+Z$  direction, it is clear in (f) that both the tapered fiber optic tip and the silica microsphere travel together as they both leave the focal point of the microscope, returning to the focal point in (g) when moved in the  $-Z$  direction. Thus, it is evident that the sphere is confined and manipulated in a gradient force 3-D optical trap.

#### 5 Investigation of Trapping Degradation at Sub-45-Deg Insertion Angles

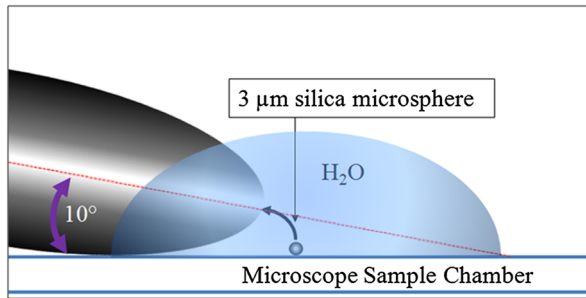
When the insertion angle for tip number 44 was altered from 45 to 10 deg, it was found that 3-D optical trapping could only be realized at an extremely high optical power output, which was in excess of 500 mW. It was this observation that led to the following hypothesis regarding a single fiber optical trap's inability to trap below 20 deg.

Figure 5 portrays a tapered optical fiber tip incident on the microscope sample chamber at an insertion angle of 45 deg. Once the fiber taper is sufficiently elevated, it sits directly above the subject microsphere allowing easy 3-D trapping to occur.

The implications of adopting such a short tapered, large-diameter tip at an insertion angle of 10 deg can be seen in Fig. 6. The underlying problem is that the fiber is now at an almost parallel plane to the microscope sample chamber.



**Fig. 5** Large diameter, tapered optical fiber tip at an insertion angle of 45 deg.



**Fig. 6** Large-diameter tapered optical fiber tip at an insertion angle of 10 deg.

This combination constitutes a fiber tip geometry for which the trapping zone is significantly elevated above the surface of the sample chamber’s base surface. The result of this is that the microsphere has to be significantly elevated in the vertical +Z direction to enter the trapping zone. Unsurprisingly, this can only be achieved through the generation of very high optical forces, which are not acceptable for use in cell trapping applications such as the one envisaged here, as they result in cell damage.

**5.1 Fiber Taper Optimization for 3-D Optical Trapping at a 10-Deg Insertion Angle**

For biological samples, such as cells, to maintain viability during optical trapping procedures, typical optical powers employed can be as high as 340 mW at a wavelength ( $\lambda$ ) of 1064 nm and depend on the experiment conducted.<sup>51</sup> Therefore, increasing the optical power beyond this value is not a viable solution. Initial tests show that it would take focused laser light with optical powers in excess of 500 mW to 3-D optically trap at an insertion angle of 10 deg using tip number 44.

An alternative method to increase the optical forces being produced would be to optimize the laser beam’s focus. This, in turn, would generate a steeper intensity gradient and, thus, facilitate an increased gradient force. This could be achieved by altering the geometric profile of the tapered optical fiber tip. Furthermore, shaping the taper profile in such a way as to coerce the laser beam’s focal point closer to the subject to be trapped could also aid optical trapping. This action would potentially offer a superior and cell safe alternative to simply increasing the optical output power. Such a fiber taper would be required to exhibit a longer taper length and a reduction in tip diameter similar to that portrayed in Fig. 7.

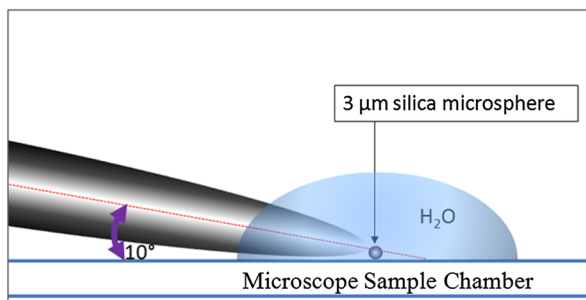


**Fig. 7** Proposed optimized optical fiber taper geometry possessing a longer taper length combined with a smaller diameter tip to gain closer proximity to the sample.

However, this type of taper profile could also prove to be unfeasible, since the long-taper, small-diameter tip may result in the fiber losing its integrity. This would inherently lead to the fiber becoming predisposed to high optical losses at the tapered tip. Such losses would effectively reduce the taper’s ability to efficiently transport the laser light along the entirety of the taper due to TIR. Such losses would hinder the tapered fiber tip’s ability to focus the light and, therefore, its ability to form an effective optical trap.

**5.2 Development of Fiber Tapers for Optical Trapping at a 10-Deg Insertion Angle**

Three additional working tips, numbered 92, 94, and 96, respectively, were successfully developed in an attempt to increase the likelihood of 3-D trapping at an insertion angle of 10 deg. The parameter values for the P2000/F programs can be seen in Table 2. Each of the tips underwent and passed the required 3-D optical trapping test as previously discussed in Sec. 4. Figures 8(b) to 8(d) show the dimensions of the three new tips, numbered 92, 94, and 96, in comparison with the original tip number 44 in Fig. 8(a).

**Table 2** Parameter values for the P2000/F micro-pipette puller used to fabricate the optical fiber tapers.

Program number	Heat	Filament	Velocity	Delay	Pull
44	320	002	022	128	000
	320	002	022	128	175
92	340	002	023	128	000
	340	002	023	127	175
94	325	002	023	128	000
	325	002	023	127	175
96	320	002	023	128	000
	320	002	023	127	175

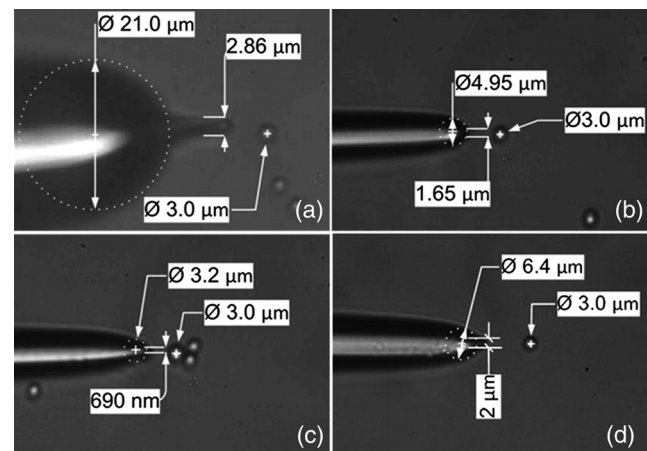


**Fig. 8** Dimensions of the tapered fiber optic tips numbered (a) 44, (b) 92, (c) 94, and (d) 96.

## 6 3-D Optical Trapping Test at 10-Deg Insertion Angle

Each of the three new tips demonstrated 3-D optical trapping of 3- $\mu\text{m}$ -diameter silica microspheres at an insertion angle of 10 deg to the microscope sample chamber. Each of the optimized optical fiber tapers could elevate and hold 3- $\mu\text{m}$ -diameter silica microsphere using optical powers as low as 10 mW. The microsphere could remain elevated by the optical trap after reducing the optical powers down to 1 mW.

### 6.1 Change in Trap Dynamics

When compared to optical trapping at an insertion angle of 45 deg, trapping at an insertion angle of 10-deg bore witness to changes in the trapping dynamics. First, while optical trapping at an insertion angle of 45 deg, it is difficult to trap and isolate a single particle. There is a tendency for multiple particles to be drawn into the optical trap. However, at an insertion angle of 10 deg, only a single particle could usually be trapped, with any additional particles being propelled in the direction of the beam. However, occasionally, two or three particles were observed to be simultaneously trapped.

The second change can be seen in Fig. 9, in which the introduction of a maximum trapping range (MTR) is depicted. The MTR comes into effect and is observable as the fiber is closer to a horizontal orientation. Therefore, there is no longer the same physical impedance provided by the glass microscope sample slide.

The image shows that there is a point at which the gradient and scattering forces cancel each other out, resulting in a zero net force. To either side of this equilibrium point are areas where either gradient or scattering forces dominate, respectively, and a particle's position in one or the other of these two areas dictates the direction in which the particle will subsequently move. If the particle is located on the side characterized by a dominant gradient force, then the particle is attracted toward the focal point of the laser beam and becomes optically trapped. If the particle is located toward the side characterized by a dominant scattering force, then the particle is repelled.

### 6.2 Experimental Method for Determining the Maximum Trapping Range

Discovery of a given taper's MTR was achieved by first optically trapping the subject microsphere as depicted in Fig. 10 (top). The laser is then deactivated and the optical fiber taper is moved a short distance in the negative  $X$  direction as depicted in Fig. 10 (middle). This short distance must be

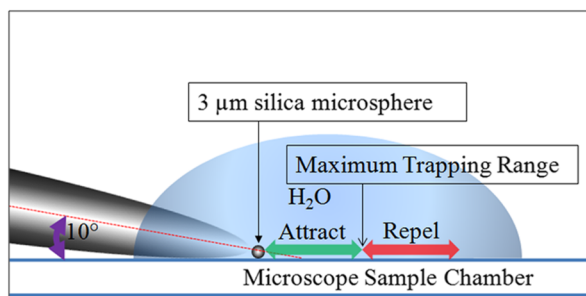


**Fig. 9** Change in trapping dynamics with the introduction of a maximum trapping range.

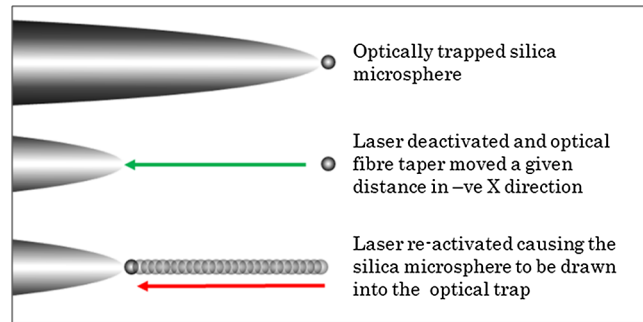


**Fig. 10** Experimental procedure carried out to determine the trapping range.

less than the yet unknown maximum trapping range to ensure retrapping of the microsphere. When the tapered optical fiber occupies its new position, the laser is reactivated and the microsphere is attracted to the trapping zone as shown in Fig. 10 (bottom).

Initially, the distance between the tapered optical fiber's tip and the sphere is relatively short in order to establish a base point. If the distance is too great, the particle is repelled as it sits beyond the maximum trapping range. When the base point has been established, the process of trapping from a distance is repeated. Each time the process is repeated, the negative  $X$  distance of the optical fiber taper is systematically increased by 1- $\mu\text{m}$  increments from the established base point. At the point at which trapping no longer occurs and the microsphere is repelled, the previous distance is deemed to be the extremity of the maximum trapping range.

Videos of the optical trapping procedures are recorded and analyzed using a particle tracking (PT) software package which tracks the particle's course through each frame of video. The PT software calculates the coordinate data in both pixel and real distance values for the particle's trajectory along with the associated timestamps to enable further velocity and force analysis.

When attempting to determine the trapping range, a discrepancy was noted. It was found after running the associated video data through the PT software. The experimental data showed that the actual distance the particle travelled did not correctly correspond with the distance that the optical fiber taper was moved in the negative  $X$  direction, as determined by the Piezo translation monitoring and control software.

To further investigate this apparent anomaly, the experiment was repeated for a predetermined distance. The fiber was moved in the negative  $X$  direction away from the previously trapped microsphere by a distance of 9  $\mu\text{m}$  for tapers 92 and 94, and 10  $\mu\text{m}$  for taper 96. On each occasion, the microsphere's path back into the optical trapping zone was recorded using a high-speed video camera for later analysis using the PT software.

After comparison of the associated PT and Piezo monitoring and control data, a displacement error was determined, as shown in Table 3. To test that the discrepancy was not due to the Piezo actuator not translating for the required distance, a further check was made. This involved a 3- $\mu\text{m}$  silica microsphere being optically trapped and the fiber being moved in the negative  $X$  direction by a distance of 10  $\mu\text{m}$ , while the silica microsphere was still under the

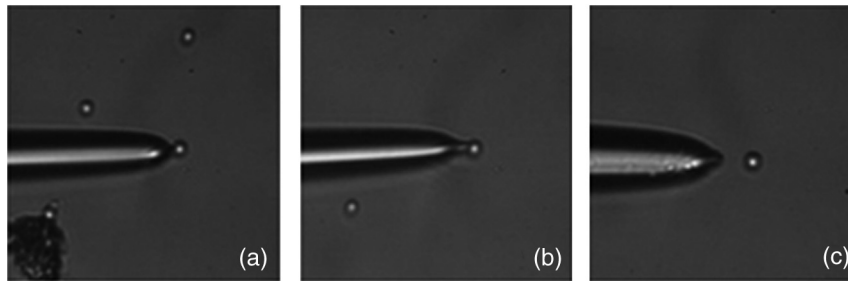


**Fig. 11** Tapered optical fiber tips optically trapping 3- $\mu\text{m}$  silica microspheres showing their trapping zones corresponding to program numbers (a) 92, (b) 94, and (c) 96.

influence of the optical forces. The associated video data were then passed through the PT software and the distance travelled by the microsphere was found to be equal to the distance of the Piezo translation, thus eliminating any possibility of Piezo error.

### 6.3 Results: Determining the Maximum Trapping Range

Figures 11(a), 11(b), and 11(c) show the three optimized tapered optical fiber tips numbered 92, 94, and 96, respectively. It can be seen that for tips numbered 92 and 94, the focal points or trapping zones are in similar locations. Both can be seen to be trapping a 3- $\mu\text{m}$  silica microsphere at the fiber end with the microsphere actually coming into contact with the tip of the optical fiber. In contrast, the trapping zone for the tapered optical fiber tip numbered 96 can be seen to be at a distance of  $\sim 6.5 \mu\text{m}$  away from the end of the optical fiber tip.

Table 3 shows that the maximum trapping range for the three optical fiber tapers were found to be 9, 13, and 13  $\mu\text{m}$  for the optical fiber tapered tips 92, 94, and 96, respectively. However, in the case of tip number 96, the actual maximum distance from the end of the tapered optical fiber, from which a particle can be drawn into the optical trap is 19.5  $\mu\text{m}$ . This is due to the trapping zone or the focal point being located 6.5  $\mu\text{m}$  from the taper's end.

The disparity between the distance that the tapered optical fiber was moved in the negative X direction and the actual distance that the particle was displaced when being drawn back toward the fiber tip and into the optical trap can be seen in Table 3. It shows that there is a displacement error associated with the compared values. Tapered tip number 96 is seen to have the least error with 18% error, compared with 30.3 and 32.1% errors for tips 92 and 94, respectively.

**Table 3** Trapping range error.

P2000/F program number	92	94	96
Maximum trapping range ( $\mu\text{m}$ )	9	13	13
Tip movement piezo value ( $\mu\text{m}$ )	9	9	10
Particle movement particle tracking value ( $\mu\text{m}$ )	6.27	6.11	8.20
Percentage error %	30.3	32.1	18

## 7 Trapping of Organic Material

Silica microspheres provide a good optical trapping subject that is ideal for system characterization. The reason for this is their uniformity in size, shape, and optical characteristics, i.e., refractive index. Live biological materials, such as cells, are dynamic. They can change shape and grow. Their optical characteristics are complex since their makeup consists of many dynamic components and materials. Therefore, optical fiber tips that are suitable for the trapping of silica microspheres might not be suitable for the trapping of complex biological systems.

The three tapered tips were tested to see if they could optically trap yeast cells in 3-D. This is by no means a thorough examination, since there are many different cells of all shapes and sizes which will be featured during future work. All three tips successfully trapped and elevated yeast cells of  $\sim 6 \mu\text{m}$  in diameter as shown in Fig. 12, where the fiber tip and the optically trapped yeast cell are both in focus and elevated above the general population of yeast cells. The nucleus of the trapped yeast cell is clear. Since the untrapped yeast cells are not in the focus of the microscope objective, they are seen as the dark shadow-like features.

## 8 Discussion

Three optimized optical fiber tapered tips have been developed for optical trapping at extremely shallow insertion angles of  $\leq 10$  deg. This orientation can be considered to be nearly horizontal and almost parallel to the plane of the sample chamber's base. All three of the optimized tapers could successfully trap, elevate, and hold 3- $\mu\text{m}$  silica microspheres using as little as 1 mW of optical power, a significant improvement compared with the original optical fiber taper number 44 that required in excess of 500 mW in order to trap



**Fig. 12** Optical trapping and elevation of a yeast cell.

a similar silica microsphere in 3-D at an insertion angle of 10 deg.

The result of being able to trap at low optical powers is that the system is ideally suited for the optical trapping of organic biological material. The fact that optical trapping at low powers can now occur at insertion angles of  $\leq 10$  deg offers proof of concept that the fiber based optical trapping system developed here can be successfully integrated with an AFM. However, further work is still required before this realization can be implemented. For example, an IR optical filter would have to be retro-fitted in order to block the scattered optical trapping laser light from interfering with the AFM head optical lever detection system.

The contrast in maximum trapping ranges for the three optimized optical fiber tapered tips suggests that the maximum trapping range is tunable and is dependent upon the geometrical profile of the optical fiber taper. Furthermore, the trapping range can be exploited to offer a solution to particle sorting. The reduction in the optical trapping volume associated with near horizontal trapping at an insertion angle of 10 deg compared to trapping at a 45-deg insertion angle, will potentially offer a great advantage for applications involving single cell manipulation or particle sorting.

The observation that the distances are unequal for the optical fiber movement in the negative  $X$  direction and the actual particle displacement as it is drawn into the optical trap, can be explained through the following hypothesis. When the taper is moved away from the microsphere, the relatively large size and shape of the optical fiber taper causes a disturbance in the medium. The microsphere, which is then free from optical trapping forces, is then dragged in the tapered optical fibers wake, i.e., the disturbance within the medium caused by the relatively large tapered optical fiber's physical movement. Therefore, the microsphere's original position is not maintained. This phenomenon is compounded as the effects of Brownian motion may also contribute to the microsphere's new starting point.

This hypothesis is strongly supported as it is evident that the percentage error for taper 96 is far less than that of tapers 92 and 94. This can be attributed to the focal point of taper 96 being a distance of  $\sim 6.5 \mu\text{m}$  away from the fiber end-face, unlike that of tapers 92 and 94, both of which have a trapping point that is in extreme close proximity (equal to the radius of a microsphere  $\approx 1.5 \mu\text{m}$ ) to the end of the tapered tip. Consequently, any potential tip disturbance effects for tapered optical fiber tip numbered 96 would impinge less upon the microsphere as it is at a greater distance from the tip in comparison to tapered optical fiber tips numbered 92 and 94.

The maximum trapping ranges offered by the three optimized tapered fiber optic tips numbered 92, 94, and 96 are given as 9, 13, and 13  $\mu\text{m}$ , respectfully. The measured values are in good agreement with the simulated data presented in Ref. 10, in which the predicted values for the trapping range of a tapered optical fiber were stated to be in the range of 0 to 12  $\mu\text{m}$ . However, this simulated data suggested that particles located at a distance of 15  $\mu\text{m}$  from the optical fiber would be propelled away from the tip due to the scattering force. This simulation implies then that there is a 3  $\mu\text{m}$  distance between 12 and 15  $\mu\text{m}$  from the fiber tip over which it is not clear whether a particle would be either trapped or repelled.

Here the authors have experimentally determined the maximum trapping range to an accuracy of 1  $\mu\text{m}$ . Such accuracy was achieved as the incremental distances that the fiber was moved away from the particle were 1  $\mu\text{m}$  in length. Taking into account the simulated data's uncertainty of 3  $\mu\text{m}$ , the accuracy provided by the 1- $\mu\text{m}$  increments was deemed satisfactory.

The trapping region of tip number 96 is also of great interest as its distance from the tip is ideally suited for noncontact manipulation of larger and biological material since the physical optical fiber would not cause interference with the specimen.

It is believed that the variances in maximum trapping range could also offer an indication as to the quality of the optical trapping efficiency, the reasoning being that increases in trapping ranges could be due to increases in the gradient forces being generated through optimized focusing of the beam.

## 9 Conclusion

The literature suggests that single optical fiber 3-D optical trapping systems cannot operate at fiber insertion angles of  $< 20$  deg. In order for a single fiber based system to be integrated within an AFM, this assumption must be contradicted; otherwise the amalgamation of the two systems cannot be realized. The reason is that in order for the fiber to pass under the AFM head, it must enter the sample chamber at an insertion angle of 10 deg.

A comprehensive review of the various optical trapping system configurations that are currently available and a description of the tapered fiber optic tweezers (T-FOT's) system developed here is presented. This is followed by an investigation as to why optical trapping, for single fiber based systems, fails at low insertion angles and a hypothesis based on the findings is offered.

The investigations found that the geometric profile of the tapered optical fiber tip number 44 was too large. The result of this meant that any potential trapping targets would have to be elevated up into the trapping zone. This required in excess of 500 mw of optical power and was, therefore, unfeasible as such high intensities would be highly damaging to living biological samples. This finding led to the development of three optimized optical fiber taper profiles. Consisting of longer taper lengths and reduced tip diameters. By using these optimized tapers, 3-D optical trapping at an insertion angle of 10 deg and with reduced optical power outputs of a little as 1 mW was achieved. The results offer proof of concept that the T-FOT's system could be successfully integrated with a typical AFM, subject to modifications being made to protect its optical lever detection system from the trapping laser.

When compared to optical trapping at a 45-deg insertion angle, optical trapping at the near horizontal insertion angle of 10 deg produced a change in the optical trapping dynamics.

First, there was the introduction of a maximum trapping range, which is the maximum distance from the focal point or trapping zone in which the particle can be drawn in and trapped. Beyond this point the particle is repelled due to the influence of the greater scattering force. The maximum trapping ranges for the tips numbered 92 and 94 are both given as 9  $\mu\text{m}$  and that for tip number 96 is 13  $\mu\text{m}$ . Such variances in

the maximum trapping ranges of the optimized tapered optical fiber tips suggest that the maximum trapping range is tunable, is dependent on the geometric profile of the optical fiber taper, and could possibly be an indicator for trapping efficiency.

Second, the trapping volume was found to be substantially reduced in that only a single particle could be trapped at any one time. Being able to target a specific particle in this manner could be used for single particle analysis and particle sorting applications.

Finally, the optimized tapers also exhibited varying focal distances from the end of the optical fiber tip. Tips 92 and 94 both trapped the particle at the end of the fiber at a distance equal to the radius of the microsphere. Tip 96, on the other hand, trapped a particle  $\sim 6.5 \mu\text{m}$  away from the tip's end-face, which could be exploited for noncontact manipulation of biological cells, or large-diameter targets.

### Acknowledgments

This research was supported by the Engineering and Physical Sciences Research Council (EPSRC) under Grant No. R66311G. The authors thank EPSRC, Engineering Instrument Loan Pool, Rutherford Appleton Laboratory, United Kingdom, for the loan of the Photron FASTCAM MC-1 and the Photron Ultima APX, CMOS high-speed video cameras.

### References

1. A. Doyle et al., "Actin bundling and polymerisation properties of eukaryotic elongation factor 1 alpha (eEF1A), histone H2A-H2B and lysozyme in vitro," *J. Struct. Biol.* **176**(3), 370–378 (2011).
2. G. Johnston et al., "Analysis of microscopy and reconstructive images for applications in medicine and biology," in *18th IEEE Int. Conf. on Image Processing*, Brussels, pp. 3069–3072, IEEE (2011).
3. M. F. Murphy, "Investigating the mechanical & structural properties of human cells using atomic force & confocal microscopy," PhD Thesis, General Engineering Research Institute, Liverpool John Moores University, Liverpool (2007).
4. M. F. Murphy et al., "Comparative study of the conditions required to image live human epithelial and fibroblast cells using atomic force microscopy," *Microsc. Res. Tech.* **69**(9), 757–765 (2006).
5. M. F. Murphy et al., "Evaluation of a nonlinear Hertzian-based model reveals prostate cancer cells respond differently to force than normal prostate cells," *Microsc. Res. Tech.* **76**(1), 36–41 (2013).
6. C. M. Randall, "Investigating the mechanical and structural properties of human cells by atomic force microscopy," PhD Thesis, General Engineering Research Institute, Liverpool John Moores University, Liverpool (2009).
7. K. Taguchi et al., "Three-dimensional optical trapping for cell isolation using tapered fiber probe by dynamic chemical etching," *J. Phys.: Conf. Ser.* **352**(1), 012039 (2012).
8. Z. Hu, J. Wang, and J. Liang, "Manipulation and arrangement of biological and dielectric particles by lensed fiber probe," *Opt. Express* **12**(17), 4123–4128 (2004).
9. G. Brambilla and F. Xu, "Adiabatic submicrometric tapers for optical tweezers," *Electron. Lett.* **43**(4), 204–206 (2007).
10. Z. Liu et al., "Tapered fiber optical tweezers for microscopic particle trapping: fabrication and application," *Opt. Express* **14**(25), 12510–12516 (2006).
11. A. Ashkin, "Acceleration and trapping of particles by radiation pressure," *Phys. Rev. Lett.* **24**(4), 156–159 (1970).
12. A. Ashkin and J. M. Dziedzic, "Optical levitation by radiation pressure," *Appl. Phys. Lett.* **19**(8), 283–285 (1971).
13. A. Ashkin et al., "Observations of a single-beam gradient force optical trap for dielectric particles," *Opt. Lett.* **11**(5), 288–290 (1986).
14. D. G. Grier and Y. Roichman, "Holographic optical trapping," *Appl. Opt.* **45**(5), 880–887 (2006).
15. E. R. Dufresne and D. G. Grier, "Optical tweezer arrays and optical substrates created with diffractive optics," *Rev. Sci. Instrum.* **69**(5), 1974 (1998).
16. M. Capitano, R. Cicchi, and F. S. Pavone, "Continuous and time-shared multiple optical tweezers for the study of single motor proteins," *Opt. Lasers Eng.* **45**(4), 450–457 (2007).
17. K. Visscher, G. J. Brakenhoff, and J. J. Krol, "Micromanipulation by 'multiple' optical traps created by a single fast scanning trap integrated with the bilateral confocal scanning laser microscope," *Cytometry* **14**(2), 105–114 (1993).
18. K. Visscher, S. P. Gross, and S. M. Block, "Construction of multiple-beam optical traps with nanometer-resolution position sensing," *IEEE J. Sel. Topics Quantum Electron.* **2**(4), 1066–1076 (1996).
19. E. Fallman and O. Axner, "Design of a fully steerable dual-trap optical tweezers," *Appl. Opt.* **36**(10), 7 (1997).
20. H. Misawa et al., "Multibeam laser manipulation and fixation of microparticles," *Appl. Phys. Lett.* **60**(3), 310–312 (1992).
21. G. V. Soni et al., "Development of an optical tweezer combined with micromanipulation for DNA and protein nanobioscience," *Curr. Sci.* **83**(12), 1464–1470 (2002).
22. D. G. Grier, "A revolution in optical manipulation," *Nature* **424**(6950), 810–816 (2003).
23. A. Ashkin, "Trapping of atoms by resonance radiation pressure," *Phys. Rev. Lett.* **40**(12), 729–732 (1978).
24. S. Kawata et al., "Finer features for functional microdevices," *Nature* **412**(6848), 697–698 (2001).
25. A. Ashkin and J. M. Dziedzic, "Optical trapping and manipulation of viruses and bacteria," *Science* **235**(4795), 4 (1987).
26. A. Ashkin and J. M. Dziedzic, "Internal cell manipulation using infrared laser traps," *Proc. Natl. Acad. Sci.* **86**(20), 7914–7918 (1989).
27. A. Ashkin, J. M. Dziedzic, and T. Yamane, "Optical trapping and manipulation of single cells using laser beams," *Nature* **330**(24), 3 (1987).
28. A. Ashkin et al., "Force generation of organelle transport measured in vivo by an infrared laser trap," *Nature* **348**(6299), 346–348 (1990).
29. A. Ashkin, "Forces of a single-beam gradient laser trap on a dielectric sphere in the ray optics regime," *Biophys. J.* **61**(2), 569–582 (1992).
30. A. Ashkin, "Optical trapping and manipulation of neutral particles using lasers," *Proc. Natl. Acad. Sci.* **94**(10), 4853–4860 (1997).
31. K. Svoboda and S. M. Block, "Biological applications of optical forces," *Annu. Rev. Biophys. Biomol. Struct.* **23**, 247–285 (1994).
32. G. J. Brouhard et al., "Advanced optical tweezers for the study of cellular and molecular biomechanics," *IEEE Trans. Biomed. Eng.* **50**(1), 121–125 (2003).
33. K. C. Neuman and S. M. Block, "Optical trapping," *Rev. Sci. Instrum.* **75**(9), 23 (2004).
34. N. Malignino et al., "Measurements of trapping efficiency and stiffness in optical tweezers," *Opt. Commun.* **214**(1–6), 15–24 (2002).
35. A. Constable et al., "Demonstration of a fiber optical light-force trap," *Opt. Lett.* **18**(21), 1867–1869 (1993).
36. E. R. Lyons and G. J. Sonek, "Confinement and bistability in a tapered hemispherically lensed optical fiber trap," *Appl. Phys. Lett.* **66**(13), 1584 (1995).
37. K. Taguchi et al., "Levitation of a microscopic object using plural optical fibers," *Opt. Commun.* **176**(1–3), 43–47 (2000).
38. K. Taguchi, M. Tanaka, and M. Ikeda, "Theoretical study of an optical levitation using dual beam from optical fibres inserted at an angle," *Opt. Commun.* **194**(1–3), 67–73 (2001).
39. M. Ikeda et al., "Rotational manipulation of a symmetrical plastic micro-object using fiber optic trapping," *Opt. Commun.* **239**(1–3), 103–108 (2004).
40. S. D. Collins, R. J. Bashkin, and D. G. Howitt, "Microinstrument gradient-force optical trap," *Appl. Opt.* **38**(28), 6068–6074 (1999).
41. S. D. Collins et al., "Micromachined optical trap for use as a micro-cytology workstation," *Proc. SPIE* **2978**, 69–74 (1997).
42. R. Taylor and C. Hnatovsky, "Particle trapping in 3-D using a single fiber probe with an annular light distribution," *Opt. Express* **11**(21), 2775–2782 (2003).
43. Z. Hu, J. Wang, and J. Liang, "Manipulation of yeast cells by a tapered fiber probe and measurement of optical trapping force," *J. Korean Phys. Soc.* **47**, S9–S12 (2005).
44. S. Cabrini et al., "Axicon lens on optical fiber forming optical tweezers, made by focused ion beam milling," *Microelectron. Eng.* **83**(4–9), 804–807 (2006).
45. C. Liberale et al., "Minaturised all fiber probe for three dimensional optical trapping and manipulation," *Nat. Photonics* **1**(12), 723–727 (2007).
46. P. Minzioni et al., "A novel approach to fiber-optic tweezers: numerical analysis of the trapping efficiency," *IEEE J. Sel. Topics Quantum Electron.* **14**(1), 151–157 (2008).
47. F. Bragheri et al., "Numerical and experimental demonstration of a single fiber for optical trapping and analysis," in *Lasers and Electro-Optics/Quantum Electronics and Laser Science Conference and Photonic Applications Systems Technologies*, San Jose, California, pp. 1–2, Optical Society of America (2008).
48. F. Bragheri et al., "Design and optimisation of a reflection based fiber optical tweezers," *Opt. Express* **16**(22), 17647–17653 (2008).
49. L. Yuan et al., "Twin core fiber optical tweezers," *Opt. Express* **17**(7), 4551–4558 (2008).
50. G. Zhang et al., "Numerical analysis of near-field optical trapping using tapered fiber probe," *Proc. SPIE* **4082**, 321–328 (2000).

51. S. P. Gross, "Application of optical traps in vivo," in *Methods in Enzymology*, M. Gerard and P. Ian, Eds., pp. 162–174, Academic Press, Miamisburg, OH (2003).

**Steven Ross** is a PhD student and a member of the Cell Mechanics Group, which is a multidisciplinary team of engineers and life scientists at the General Engineering Research Institute, Liverpool John

Moores University. Research interest in optical fiber based optical trapping—optical tweezers. He received an MSc in telecommunications engineering from Liverpool John Moores University (LJMU) in 2007 with a BEng in electronics and communications engineering also from LJMU in 2005.

Biographies of the other authors are not available.